JOURNAL OF COMPUTATIONAL PHYSICS 31, 363–378 (1979)

Separating Boundary-Layer Flow Calculations*

T. CEBECI

Mechanical Engineering Department, California State University at Long Beach, California 90840

AND

H. B. KELLER†

Applied Mathematics, California Institute of Technology, Pasadena, California 91125

AND

P. G. WILLIAMS

Department of Mathematics, University College, London, United Kingdom

Received August 8, 1977; revised August 2, 1978

The Box scheme has been used along with the Reyhner and Flugge-Lotz approximation and a nonlinear eigenvalue approach to inverse boundary-layer flows to compute flows with separation and reattachment. The approximate reverse flow region is corrected by a downstream-upstream iteration procedure similar to that introduced by Klemp and Acrivos, but implemented quite differently, and it converges extremely fast. A careful look at the convergence properties and the occurence of very small oscillations suggests several smoothing procedures which can be used for very severe cases of reverse flow.

1. INTRODUCTION

It had long been believed that boundary-layer theory was inadequate to describe flows with separation and regions of reverse flow. Indeed it was shown by Goldstein [9] that the solution of the "standard" boundary-layer problem (i.e., pressure gradient given) may have a singularity at the point of separation. However Catherall and Mangler [5] were able to compute what seemed to be smooth solutions beyond separation. To do this they replaced the standard boundary-layer problem by a nonstandard one in which the displacement thickness is specified and the external flow velocity, or equivalently the downstream pressure gradient, is not specified. Following this basic work there have been several recent computations of laminar

* This work was supported by the Office of Naval Research under contract N00014-75-C-0607.
† Supported in part by U.S. Army Research Office under Contract DAHC-04-68-007.

0021-9991/79/060363–16$02.00/0

boundary layers with displacement thickness and shear-stress prescribed in regions where the shear-stress is negative; see, for example: Klineberg and Steger [15], Horton [10], Carter [2, 3], Carter and Wornum [4], and Williams [17, 18]. A brief clear discussion of the problem of singularities *vs* regular flow at separation is given by Brown and Stewartson [1].

In this paper we present another method, employing the Box-scheme for computing boundary layers with reverse flows for laminar situations. It is based on previous methods we have developed for what we called inverse boundary-layer problems [7, 12], and for reverse flow calculations [8, 16]. To adapt these methods to the case of reverse flow, we first make use of the approximation due to Reyhner and Flugge–Lotz [16]. This approximation, which is to drop the uu_x term wherever u becomes negative, is common to most such computations. Then we correct this approximation by a sequence of downstream-upstream iterations. We have developed two distinct techniques for solving inverse boundary-layer problems: the nonlinear eigenvalue method [12, 17] and the Mechul-function method [7, 8]. Both methods have been successful in application to separating flows. However, the eigenvalue method as formulated by Williams [17] seems to be more efficient and so we shall only describe its application here. The downstream-upstream iterations are very much in the spirit of the work of Klemp and Acrivos [14] but our implementation of their idea is quite different.

In Section 2 we formulate the standard and inverse boundary-layer problems for laminar flows. Then, in Section 3 we describe the following numerical procedures: in 3.1 the nonlinear eigenvalue method via the Box-scheme, in 3.2 the Reyhner–Flugge–Lotz approximation for reverse flows, and in 3.3 an upstream-downstream iterative procedure for improving the approximation. Some calculations using these methods on a problem introduced by Carter [3] are presented in Section 4 along with a discussion of the results. The iterations of Section 3.3 converge very fast even for cases of large reverse flow and this is one of the most attractive features of our method. The method has been used with equal success on several other reverse flow problems, but the examples of Carter seem to be the most severe test.

2. Standard and Inverse Boundary-Layer Problems

For steady incompressible plane flows the boundary-layer approximations to the Navier–Stokes equations are:

Continuity equation:

$$\frac{\partial u}{\partial x} + \frac{\partial v}{\partial y} = 0 \tag{2.1}$$

x-Momentum equation:

$$u\frac{\partial u}{\partial x} + v\frac{\partial u}{\partial y} = -\frac{1}{\rho}\frac{\partial p}{\partial x} + \frac{1}{\rho}\frac{\partial \tau}{\partial y} \tag{2.2}$$

y-Momentum equation:

$$0 = -\frac{1}{\rho}\frac{\partial p}{\partial y} \tag{2.3}$$

where

$$\tau = \rho\nu\frac{\partial u}{\partial y} \tag{2.4}$$

Obviously the approximations leading to (2.3) imply that the pressure varies only in the downstream direction, $p = p(x)$. However, the Mechul-function procedure [8] essentially neglects this fact, as far as the numerical work is concerned, and employs directly difference approximations to (2.3). We shall not use this technique in the present work.

The usual boundary conditions are, for a fixed rigid surface at $y = 0$, say:

$$u(x, 0) = v(x, 0) = 0 \tag{2.5}$$

and as the freestream is approached, $y \to y_\infty$, say

$$u(x, y_\infty) = u_e(x) \tag{2.6a}$$

Also, at the edge of the boundary layer the pressure and the free stream velocity, $u_e(x)$, must satisfy the inviscid Euler equation:

$$u_e(x)\frac{\partial u_e(x)}{\partial x} = -\frac{1}{\rho}\frac{\partial p(x, y_\infty)}{\partial x}. \tag{2.6b}$$

In "standard" problems either $u_e(x)$ or $p(x)$ is specified and then $p(x)$ or $u_e(x)$, respectively, is determined from (2.6b).

However, in our present inverse problems we specify neither $u_e(x)$ nor $p(x)$, but rather the displacement thickness:

$$\delta^*(x) = \int_0^{y_\infty}\left[1 - \frac{u(x, y)}{u_e(x)}\right]dy. \tag{2.7}$$

By introducing a stream function we can, as usual, satisfy the continuity equation and replace the integral constraint in (2.7) by a simple boundary condition. Thus, in terms of a reference length, L, and a velocity, u_0, we introduce the dimensionless, quantities:

$$\begin{aligned} &R \equiv u_0 L/\nu, \quad \bar{x} \equiv x/L, \quad \bar{y} \equiv yR^{1/2}/L, \quad \bar{u} \equiv u/u_0, \quad \bar{v} \equiv vR^{1/2}/u_0 \\ &\bar{p} \equiv p/\rho u_0^2, \quad \bar{u}_e \equiv u_e/u_0, \quad \bar{\delta}^* \equiv \delta^* R^{1/2}/L. \end{aligned} \tag{2.8}$$

The stream function $\psi(\bar{x}, \bar{y})$ is to be determined such that

$$\frac{\partial\psi}{\partial\bar{x}} = -\bar{v} \qquad \frac{\partial\psi}{\partial\bar{y}} = \bar{u}. \tag{2.9}$$

Then (2.1) is satisfied and with the scaling (2.8), we get from (2.2) through (2.4), using primes to denote $\bar{y}$-differentiation:

$$\psi''' + \psi'' \frac{\partial \psi}{\partial \bar{x}} - \psi' \frac{\partial \psi'}{\partial \bar{x}} = \frac{\partial \bar{p}}{\partial \bar{x}} \tag{2.10a}$$

$$\bar{p}' = 0. \tag{2.10b}$$

The boundary conditions (2.5) on the body become:

$$\psi(\bar{x}, 0) = \psi'(\bar{x}, 0) = 0 \tag{2.11}$$

The conditions (2.6) at the edge of the boundary layer become:

$$\psi'(\bar{x}, \bar{y}_\infty) = \bar{u}_e(\bar{x}) \tag{2.12a}$$

$$\bar{u}_e(\bar{x}) \frac{d\bar{u}_e(\bar{x})}{d\bar{x}} + \frac{\partial \bar{p}(\bar{x}, y_\infty)}{\partial \bar{x}} = 0. \tag{2.12b}$$

Finally, the specification of the displacement thickness (2.7) now simplifies, using $\psi(\bar{x}, 0) = 0$, to the boundary condition:

$$\psi(\bar{x}, y_\infty) = \bar{u}_e(\bar{x})[\bar{y}_\infty - \bar{\delta}^*(\bar{x})]. \tag{2.12c}$$

2.1. *"Initial" Data*

The standard problem: (2.10a) subject to (2.11) and (2.12a), or the inverse problem: (2.10a,b) subject to (2.11) and (2.12a,b,c) both require the specification of the flow field at some upstream location, say at $x = x_0$, to complete the formulation. The specified velocities must be consistent with the boundary layer equations or must come from an actual flow field. If they are not chosen with some care, then non-physical disturbances and/or spatial oscillations may occur for $x > x_0$ in the computed solutions.

Appropriate initial data are obtained by either computing them or using experimental data. For laminar flows with $u_e \sim x$ (stagnation point flow) or $u_e =$ const(flat-plate flow) we use similarity variables to generate the initial conditions. Using the new variables, in terms of those in (2.8) with the bars dropped,

$$\eta \equiv \left(\frac{u_e}{\nu x}\right)^{1/2} y, \qquad f(x, \eta) \equiv \psi(x, y)/(u_e \nu x)^{1/2} \tag{2.13}$$

the Eqs. (2.1)–(2.4) can be reduced to:

$$f''' + \frac{m+1}{2} ff'' + m[1 - (f')^2] = x[f' f'_x - f'' f_x]. \tag{2.14}$$

Here primes denote $\partial/\partial\eta$ and m is a dimensionless pressure gradient parameter defined by

$$m \equiv \frac{x}{u_e}\frac{du_e}{dx}. \tag{2.15}$$

The boundary conditions (2.5) and (2.6a) become

$$f(x, 0) = f'(x, 0) = 0; \qquad f'(x, \eta_\infty) = 1 \tag{2.16}$$

There are many accurate procedures for the numerical solution of (2.14)–(2.16) on $0 \leqslant x \leqslant x_0$, say. Then by rescaling the computed solution at $x = x_0$ to the variables in (2.8) we obtain initial data. Of course the point x_0 must be upstream of the point of separation.

3. Numerical Procedures

We first formulate the inverse problem (2.10a,b) subject to (2.11) and (2.12a,b,c) in the appropriate first order form for the application of the Box method. Dropping bars for convenience, (2.10) becomes

$$\frac{\partial\psi}{\partial y} = U, \tag{3.1a}$$

$$\frac{\partial U}{\partial y} = V, \tag{3.1b}$$

$$\frac{\partial V}{\partial y} = \theta U\frac{\partial U}{\partial x} - V\frac{\partial\psi}{\partial x} + \frac{\partial p}{\partial x}, \tag{3.1c}$$

$$\frac{\partial p}{\partial y} = 0. \tag{3.1d}$$

In (3.1c) we have introduced the coefficient θ which will be used to implement the Reyhner–Flugge–Lotz approximation. For the present we simply observe that with $\theta = 1$ the system (3.1) is equivalent to (2.10). The boundary conditions (2.11) become:

$$\psi(x, 0) = 0, \tag{3.2a}$$

$$U(x, 0) = 0; \tag{3.2b}$$

while at the edge of the boundary layer (2.12b,c) become on eliminating $u_e(x)$ by means of (2.12a):

$$U(x, y_\infty)\frac{\partial U(x, y_\infty)}{\partial x} + \frac{\partial p}{\partial x} = 0, \tag{3.3a}$$

$$\psi(x, y_\infty) = U(x, y_\infty)[y_\infty - \delta^*(x)]. \tag{3.3b}$$

Note that we now have four boundary conditions, (3.2a,b)–(3.3a,b), to go with the system of four first order equations (3.1). So our system is at least formally consistent. One of the boundary conditions (3.3a), is nonlinear but this offers no particular difficulty since the differential equations are also nonlinear. This is essentially the Mechul function formulation of our problem and in this particular case the Mechul (special unknown) function is the pressure, $p(x, y)$. Since (3.1d) implies that p is a function of x only, several alternatives to the Mechul-function approach are possible. For the extension to problems in which p does depend on y, e.g., where curvature effects are taken into account, the Mechul-function approach would appear to be particularly convenient. But for the remainder of this paper we shall use $p = p(x)$ and thus drop (3.1d).

3.1. *The Nonlinear Eigenvalue Scheme*

We first show how to solve (3.1) subject to (3.2), (3.3) over some interval, say, $[x_0, x_N]$ which does not contain a region of flow reversal or of separation and reattachment. Then the simple modifications required to include such phenomena will be introduced in Sections 3.2 and 3.3. We use the Box-scheme introduced by Keller [11] and employed to solve a variety of boundary-layer flow problems (see for instance the text of Cebeci and Bradshaw [6]). We assume known the initial data $\{\psi^0, U^0, V^0\}$ on $x = x_0$ as discussed in Section 2.1. Of course, we set $p(x_0) \equiv p^0$, a constant. Then on $x_0 \leqslant x \leqslant x_N$, $0 \leqslant y \leqslant y_\infty$ we place a possibly nonuniform net:

$$\begin{aligned} &x_0 = 0, \qquad x_n = x_{n-1} + k_n, \qquad 1 \leqslant n \leqslant N \\ &y_0 = 0, \qquad y_j = y_{j-1} + h_j, \qquad 1 \leqslant j \leqslant J; \qquad y_J = y_\infty, \end{aligned} \tag{3.4}$$

At each point (x_n, y_j) of this net we write the approximate flow quantities as $\{\psi_j^n, U_j^n, V_j^n\}$ and p^n. For any such net-function, say w_j^n, we use the following notation for averages and difference quotients:

$$[w]_{j-1/2}^n \equiv \frac{1}{2}(w_j^n + w_{j-1}^n), \qquad \left[\frac{\partial w}{\partial y}\right]_{j-1/2}^n \equiv \frac{1}{h_j}(w_j^n - w_{j-1}^n)$$

$$\left[\frac{\partial w}{\partial x}\right]_{j-1/2}^{n-1/2} \equiv \frac{1}{k_n}([w]_{j-1/2}^n - [w]_{j-1/2}^{n-1}), \quad \left[\frac{\partial w}{\partial y}\right]_{j-1/2}^{n-1/2} \equiv \frac{1}{2}\left(\left[\frac{\partial w}{\partial y}\right]_{j-1/2}^n + \left[\frac{\partial w}{\partial y}\right]_{j-1/2}^{n-1}\right)$$

$$[w]_{j-1/2}^{n-1/2} \equiv \frac{1}{2}([w]_{j-1/2}^n + [w]_{j-1/2}^{n-1}). \tag{3.5}$$

The Box scheme difference approximations to (3.1) can now be simply defined as:

$$\left[\frac{\partial \psi}{\partial y}\right]_{j-1/2}^n = [U]_{j-1/2}^n \tag{3.6a}$$

$$\left[\frac{\partial U}{\partial y}\right]_{j-1/2}^n = [V]_{j-1/2}^n \tag{3.6b}$$

$$\left[\frac{\partial (bV)}{\partial y}\right]_{j-1/2}^{n-1/2} = \theta[U]_{j-1/2}^{n-1/2}\left[\frac{\partial U}{\partial x}\right]_{j-1/2}^{n-1/2} - [V]_{j-1/2}^{n-1/2}\left[\frac{\partial \psi}{\partial x}\right]_{j-1/2}^{n-1/2} + \left[\frac{\partial p}{\partial x}\right]^{n-1/2}. \tag{3.6c}$$

The boundary conditions (3.2), (3.3) are approximated by:

$$\psi_0^n = 0 \tag{3.7a}$$

$$U_0^n = 0 \tag{3.7b}$$

$$[U]_J^{n-1/2}\left[\frac{\partial U}{\partial x}\right]_J^{n-1/2} + \left[\frac{\partial p}{\partial x}\right]^{n-1/2} = 0 \tag{3.7c}$$

$$\psi_J^n = U_J^n[y_J - \delta\ (x_n)]. \tag{3.7d}$$

For each fixed n in $1 \leqslant n \leqslant N$ the system (3.6) with $1 \leqslant j \leqslant J$ contains $3J$ equations and with the four equations in (3.7) this yields $3J + 4$ equations for as many unknowns $\{\psi_j^n, U_j^n, V_j^n\}$, $0 \leqslant j \leqslant J$ and p^n. As we shall see, p^n plays a distinguished role in the solution procedure and behaves very much as a (nonlinear) eigenvalue parameter.

Assuming all quantities known at $x = x_{n-1}$ we solve this nonlinear algebraic system by Newton's method. First we write (3.7a,b), then in order (3.6c,a,b) for $1 \leqslant j \leqslant J$ and finally (3.7c,d). Then we introduce the iterates:

$$\psi_j^{n,i+1} \equiv \psi_j^{n,i} + \delta\psi_j^{n,i}, \quad U_j^{n,i+1} \equiv U_j^{n,i} + \delta U_j^{n,i}, \quad p^{n,i+1} = p^{n,i} + \delta p^{n,i}, \quad \text{etc.}$$

into (3.6), (3.7), ordered as indicated, and drop quadratic and higher-order terms in the corrections $\delta_j^{n,i} \equiv (\delta\psi_j^{n,i}, \delta U_j^{n,i}\, \delta V_j^{n,i})^T$, $\delta p^{n,i}$. This yields a linear system of $3J + 4$ equations, the first $3J + 3$ of which can be written as

$$A^{n,i}\Delta^{n,i} = \mathbf{R}^{n,i} - \frac{\delta p^{n,i}}{k^n}\mathbf{E}. \tag{3.8a}$$

Here $A^{n,i}$ has the block tridiagonal structure:

$$A^{n,i} \equiv \begin{bmatrix} B_0^{n,i} & C_0^{n,i} & & & \\ A_1^{n,i} & B_1^{n,i} & C_1^{n,i} & & \\ & \ddots & \ddots & \ddots & \\ & & A_{J-1}^{n,i} & B_{J-1}^{n,i} & C_{J-1}^{n,i} \\ & & & A_J^{n,i} & B_J^{n,i} \end{bmatrix}. \tag{3.8b}$$

$$\Delta^{n,i} \equiv \begin{pmatrix} \delta_0^{n,i} \\ \delta_1^{n,i} \\ \vdots \\ \delta_J^{n,i} \end{pmatrix}, \qquad \mathbf{R}^{n,i} \equiv \begin{pmatrix} \mathbf{r}_0^{n,i} \\ \mathbf{r}_1^{n,i} \\ \vdots \\ \mathbf{r}_J^{n,i} \end{pmatrix}, \qquad \mathbf{E} \equiv \begin{pmatrix} \mathbf{e}_3 \\ \mathbf{e}_3 \\ \vdots \\ \mathbf{e}_3 \end{pmatrix}. \tag{3.8c}$$

with $\mathbf{e}_3^T \equiv (0, 0, 1)$.

The components of the 3×3 matrices $\{A_j^{n,i}, B_j^{n,i}, C_j^{n,i}\}$ and the inhomogeneous

3-vectors $\mathbf{r}_j^{n,i}$ can easily be determined by carrying out the above indicated procedure. They are given explicitly in Appendix I, Eqs. (A1)–(A4).

To solve (3.8a) we use block triangular decomposition. But Keller [13] has pointed out that for boundary-value problems with more boundary conditions at the front end than at the back, the elimination can be performed more efficiently by reversing the order of the equations. This is equivalent to performing on the given system a UL decomposition rather than an LU decomposition. So we factor $A^{n,i}$ in the form

$$A^{n,i} = U^{n,i}L^{n,i} \tag{3.9}$$

where $U^{n,i}$ is unit upper triangular. Then backward and forward substitutions on the vectors $\mathbf{R}^{n,i}$ and $\mathbf{E}$, yield the vectors $\mathbf{Y}^{n,i}$, $\mathbf{Z}^{n,i}$ which satisfy:

$$A^{n,i}\mathbf{Y}^{n,i} = \mathbf{R}^{n,i} \tag{3.10a}$$

$$A^{n,i}\mathbf{Z}^{n,i} = \mathbf{E} \tag{3.10b}$$

The solution of (3.8a) is given by

$$\mathbf{\Delta}^{n,i} = \mathbf{Y}^{n,i} - \frac{\delta p^{n,i}}{k^n}\mathbf{Z}^{n,i} \tag{3.11}$$

and so we need only to determine $\delta p^{n,i}$.

We recall that the linearized form of (3.7d) which is

$$\delta\psi_J^{n,i} - [y_J - \delta\ (x_n)]\,\delta U_J^{n,i} = [y_J - \delta\ (x_n)]\,U_J^{n,i} - \psi_J^{n,i} \tag{3.12}$$

has been excluded from (3.8a). Thus, using the expressions for $\delta\psi_J^{n,i}$ and $\delta U_J^{n,i}$ from (3.11) in (3.12) yields a linear equation for $\delta p^{n,i}$. The value thus determined is then used in (3.11) to give $\Delta^{n,i}$. The factorizations (3.9) and solution of (3.10a,b) are done efficiently taking full account of the zeros occurring within the 3×3 blocks of (3.8b).

In the nonlinear eigenvalue method described in [12], a different class of problems was considered (i.e., the shear stress at $y = 0$ was specified). Then we had no (3.7d) and used the extra condition at $y = 0$ to determine the pressure. This was done by a sequence of inner- and outer-iterations which are here replaced by the need to solve two linear systems in (3.10) (i.e., the equivalent of one inner and one outer iteration).

The Newton iterations are terminated at the first i-value for which

$$\| \mathbf{\Delta}^{n,i} \| = \max_{0 \leqslant j \leqslant J} \max(|\,\delta\psi_j^{n,i}\,|, |\,\delta U_j^{n,i}\,|, |\,\delta V_j^{n,i}\,|, |\,\delta p^{n,i}\,|)] \leqslant \epsilon. \tag{3.13}$$

The error tolerance, ϵ, is usually taken to be 10^{-6}. Quadratic convergence is obtained in all of our calculations, that is

$$\| \Delta^{n,i} \| \simeq \| \Delta^{n,i-1} \|^2,$$

provided the initial guess is sufficiently accurate. This is usually assured by the choice

$$\psi_j^{n,0} \equiv \psi_j^{n-1}, \quad U_j^{n,0} \equiv U_j^{n-1}, \quad V_j^{n,0} \equiv V_j^{n-1}, \quad p^{n,0} \equiv p^{n-1}; \quad 0 \leqslant j \leqslant J. \tag{3.14}$$

After the convergence test has been passed we proceed to the next downstream station, $x_{n+1} = x_n + k_{n+1}$. If reverse flow is anticipated, which can be signaled by small or negative values of V_0^n or U_1^n, we alter the procedure as indicated in Section 3.2.

3.2. *Reverse Flow: Reyhner–Flugge–Lotz Approximation*

If the flow seems about to reverse, however this is decided, we implement the Reyhner–Flugge–Lotz approximation. In effect this amounts to dropping the transport term uu_x in the x-momentum equation wherever u becomes negative. Since this is a nonlinear effect, it is done in conjunction with the Newton iterates.

Assuming we have computed the ith Newton iterate at station x_n we then perform the tests:

$$[U]_{j-1/2}^{n,i} < 0 \qquad j = 1, 2, \ldots, J. \tag{3.15}$$

If this velocity is negative for some j value, then for that value of j we set $\theta = 0$ in (3.6c) and, correspondingly, $\theta_{j-1/2}^{n,i} = 0$ in (A2) and (A5). Otherwise we simply retain $\theta = 1$. The next Newton iterate is computed with the possibly altered data, resulting from the tests (3.15), used in (3.8). The convergence tests (3.13) and the procedure for generating initial guesses (3.14) are retained unaltered. The test (3.15) can also be used to sense the onset of reverse flow. It was used in all of our calculations.

When the entire region of flow reversal has been traversed by the above procedure, it is possible to compute more accurate approximations by including the neglected momentum transport terms. This may require an additional iterative procedure and/or an altered difference scheme in which downstream data can influence upstream data, at least where $U_j^n < 0$. Such procedures have been included by Carter [3] and Williams [17]. We have adopted the DUIT scheme of Williams [17] to improve the accuracy and it is described next.

3.3. *Downstream-Upstream Iterations*

To correct the Reyhner–Flugge–Lotz approximation we use an iterative procedure. The downstream pass of the iteration seeks to solve the inverse problem as in 3.1 but in the currently determined region of reverse flow the term $U\partial U/\partial x$ is computed from data determined during the previous upstream pass. After any downstream pass, including that of Section 3.2, we can employ an upstream pass. This computation is essentially confined to the reverse flow region. Hence the sweep is in the direction of the flow and it is stable. This idea was introduced into boundary layer theory by Klemp and Acrivos [14].

More precisely, let $y = y_0(x)$ for $x_S \leqslant x \leqslant x_R$ denote the curve on which

$U[x, y_0(x)] = 0$. The Reyhner–Flugge–Lotz calculations of 3.2 yield a first approximation to $y_0(x)$ and x_R, the reattachment point. Then the upstream sweep solves, from $x = x_R$ to $x = x_S$, a standard boundary-layer problem with U specified at the nearest net point above the current $y_0(x)$ and with the pressure gradient also specified from the last downstream sweep. To solve this standard problem, only trivial modifications are required in the scheme of 3.1. First we set $\delta p^{n,i} \equiv 0$ and do not bother to compute the $\mathbf{Z}^{n,i}$. We use $\theta \equiv 1$ and the boundary condition $\delta U_{J_n} = 0$ where (x_n, y_{J_n}) is the first netpoint above $[x_n, y_0(x_n)]$. Obviously the order of the linear systems to be solved changes with the streamwise location, x_n. The Newton convergence criterion is employed as in (3.13).

The next downstream sweep starts at the x-station just above, or at, separation using the data retained there. Again when (3.15) holds, we set $\theta = 0$ but only in (3.8b), not in (3.8c). Indeed the appropriate adjustment is trivially made by including the entire term $U\,\partial U/\partial x$ in the inhomogeneous term $R^{n,i}$ of (3.8a) and computing it from the latest upstream sweep data. We use (3.13) and (3.14) unaltered in these sweeps. Of course, the pressure as well as the reverse flow boundary, $y_0(x)$, may change during the downstream sweep which is continued until reattachment occurs.

The sequence of downstream-upstream iterations is continued until some appropriate convergence criterion is satisfied. It is not clear what the most appropriate criterion would be. Some parts of the reverse flow region seem to be somewhat less well defined, but errors there do not seriously affect the forward flow; so the most reasonable criterion might be to check the profiles at reattachment, since this would assure the accuracy of initial conditions for continuing the solution downstream.

4. Results

We present here results from a series of test calculations employing the procedures of Section 3. In particular, two cases with separation and reattachment studied by Carter [3] have been examined in some detail. These laminar flows have displacement thickness distribution given by:

$$\delta^*(x) = \begin{cases} 1.7208(x)^{1/2}, & 1.0 \leqslant x \leqslant x_1\,; \\ a_0 + a_1(x - x_1) + a_2(x - x_1)^2 + a_3(x - x_1)^3, & x_1 \leqslant x \leqslant x_2\,; \\ \hat{a}_0 + \hat{a}_2(x - x_2)^2 + \hat{a}_3(x - x_2)^3, & x_2 \leqslant x \leqslant x_3\,. \end{cases} \tag{4.1}$$

Here the coefficients are

$$\begin{aligned} &a_0 = 1.7208(x_1)^{1/2}, \qquad a_1 = (0.5)(1.7208)/(x_1)^{1/2} \\ &a_2 = (0.5/\Delta_1)[6/\Delta_1(\delta^*_{\max} - a_1) - 4a_2], \quad a_3 = 2/\Delta_1{}^3[\Delta_1/2a_2 - (\delta^*_{\max} - a_1)] \\ &\hat{a}_0 = \delta^*_{\max}, \quad \hat{a}_2 = -1/\Delta_2{}^2[3(\delta^*_{\max} - 2.25)], \quad \hat{a}_3 = 1/\Delta_2{}^3[2(\delta^*_{\max} - 2.25)] \\ &\Delta = x_2 - x_1, \quad \Delta_2 = x_3 - x_2, \quad x_1 = 1.065, \quad x_2 = 1.35, \quad x_3 = 1.884. \end{aligned} \tag{4.2}$$

The first flow with $\delta^*_{max} = 5.6$, is referred to as Case A, and the second flow with $\delta^*_{max} = 8.6$, is referred to as Case B. The two displacement thickness distributions are shown in Figures 1 and 2.

Comparison of the present use of the Reyhner–Flugge–Lotz approximation with those of Carter [3] is shown in Figures 1 and 2. The present calculations were started at $x = 0$ by solving the governing equations in transformed variables for the standard problem. Then at $x = 1$ the method of Section 3.2 was used to solve the inverse

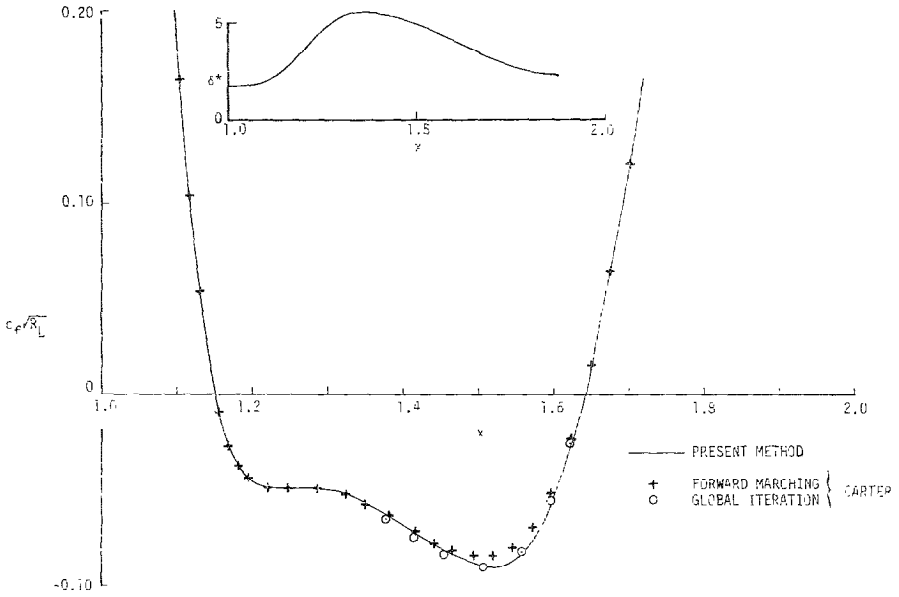

FIG. 1. Local skin-friction distribution for Case A.

problem with the equations expressed in physical variables. As can be seen, the present results agree well with those of Carter. Of course the way in which Carter implemented the Reyhner–Flugge–Lotz approximation is slightly different from that used here. The computer time was less than 10 seconds on a CDC 6600 for our fine grid of over 21,000 points ($\Delta x = 0.005$, $\Delta y = 0.1$). At all x-stations, including regions of separated flow, the convergence was quadratic and required only two to four iterations for both cases. The observed error at the termination of the iterations was 10^{-8}. Carter required an average of 14 and 28 iterations, at each x-station for cases A and B, respectively.

We also applied the downstream-upstream iteration scheme described in Section 3.3 to the cases A and B considered by Carter. The case B is obviously more severe, but the difference between the two cases does seem to be more marked than the ratio 8.6/5.6 of the peak displacement thicknesses might suggest.

Table I illustrates the rapid convergence of the scheme for case A. Typical skin-friction values in the reverse flow region are given for successive downstream and

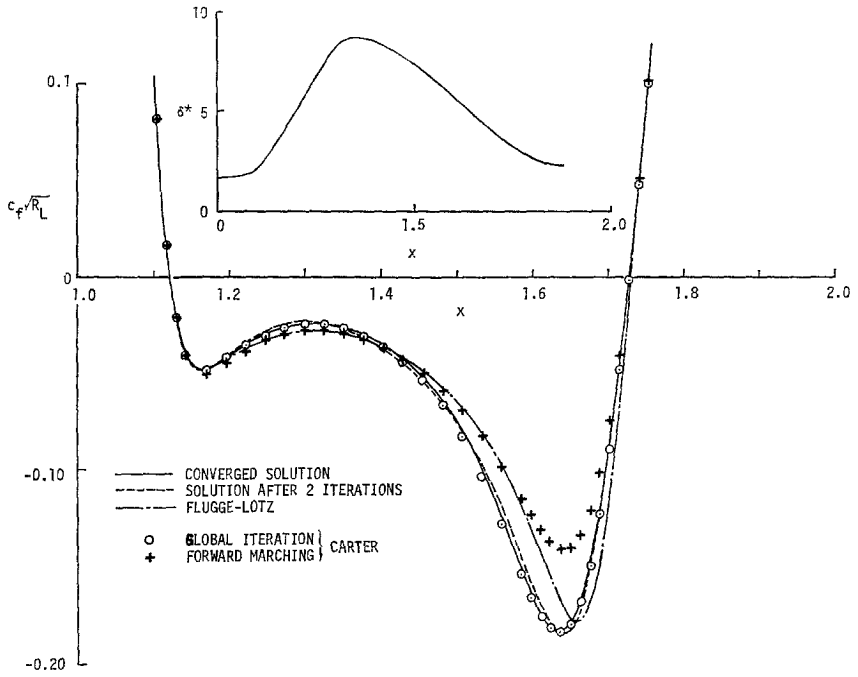

FIG. 2. Local skin-friction distribution for Case B.

TABLE I

Convergence of Negative Skin-Friction Values for Carter Case A

NODS	$x = 1.2$	$x = 1.3$	$x = 1.4$	$x = 1.5$	$x = 1.6$
0	0.0449	0.0496	0.0679	0.0881	0.0560
	0.0458	0.0525	0.0689	0.0855	0.0543
1	0.0453	0.0492	0.0704	0.0900	0.0529
	0.0451	0.0495	0.0709	0.0895	0.0530
2	0.0452	0.0492	0.0706	0.0902	0.0529
	0.0452	0.0489	0.0707	0.0901	0.0529
3	0.0452	0.0492	0.0706	0.0903	0.0529

upstream sweeps computed with $\Delta x = 0.01$, $\Delta y = 0.2$, $y_{\max} = 12$. NODS stands for the number of downstream sweeps with the initial Reyhner–Flugge–Lotz sweep counted as zero, thus the NODS count gives the number of *pairs* of up-down sweeps after the initial approximations. The rows without a NODS count give the values obtained in the upstream sweeps; the converged results are indistinguishable from

Carter's global iteration results in Fig. 1. We note that Carter required 114 of his global iterations for this case (on a fine grid).

A phenomenon which cannot be seen from the sample values is the occurrence of very small oscillations in the x-direction. They are negligible to graphical accuracy, and could not be shown in Fig. 1. But differencing to four decimals showed that for NODS = 0, their magnitude was largest near separation and decayed slowly, whereas for the converged solution their magnitude had been reduced considerably near separation but had become more marked towards reattachment.

When case B was attempted with the same step lengths, a higher NODS count was needed but also the oscillations were larger. Halving the step lengths in each direction reduced the magnitude of the oscillations considerably, and did not appear to affect the rate of convergence. Thus the oscillations are not due to numerical instabilities. Table II gives some typical values of the skin friction obtained in successive downstream and upstream sweeps with $\Delta x = 0.005$, $\Delta y = 0.1$, $y_{\max} = 15$.

It would appear that over most of the range these values have settled to three decimals and perhaps almost to four, except that the peak near reattachment is still steepening up. These values are, in fact, hardly distinguishable from Carter's graphical

TABLE II

Convergence of Negative Skin-Friction Values for Carter Case B

NODS	$x = 1.2$	$x = 1.3$	$x = 1.4$	$x = 1.5$	$x = 1.6$	$x = 1.7$
0	0.0418	0.0282	0.0364	0.0643	0.1339	0.1195
	0.0475	0.0338	0.0442	0.0717	0.1315	0.1122
1	0.0383	0.0234	0.0384	0.0741	0.1537	0.0972
	0.0347	0.0266	0.0427	0.0782	0.1520	0.0982
2	0.0403	0.0231	0.0380	0.0767	0.1607	0.0927
	0.0390	0.0225	0.0397	0.0789	0.1591	0.0933
3	0.0403	0.0233	0.0370	0.0774	0.1638	0.0917
	0.0411	0.0216	0.0376	0.0785	0.1624	0.0920
4	0.0400	0.238	0.0363	0.0772	0.1653	0.0916
	0.0408	0.0222	0.0363	0.0780	0.1646	0.0917
5	0.0398	0.0242	0.0358	0.0770	0.1664	0.0917
	0.0401	0.0230	0.0356	0.0776	0.1661	0.0917
6	0.0398	0.0244	0.0355	0.0768	0.1672	0.0916
	0.0397	0.0236	0.0353	0.0773	0.1672	0.0916
7	0.0398	0.0243	0.0354	0.0767	0.1678	0.0913

results based on his global iteration procedure which required 166 iterations. At this stage the oscillations in the x-direction would be just noticeable to graphical accuracy. However, if the downstream-upstream sweeps are continued, although the peak values near separation seem to settle down, eventually the magnitude of the oscillations increases. This is most noticeable near $x = 1.3$, where the skin friction has a negative maximum, i.e., where the reverse flow is closest to separating again. Indeed, extrapolating on the two cases, A and B, it would not be surprising if a further eddy appeared with a relatively small increase in $\delta^*_{\max}$, so that it is not unreasonable to suppose that this would be a highly sensitive region. The oscillations can be avoided by smoothing before each sweep. However, although the convergence of the downstream sweeps is then much more convincing, as also is the convergence of the upstream sweeps, they converge to slightly different limits about 0.001 apart. The average of these two limits is not necessarily more accurate since the smoothing tends to depress the build-up of the large gradients in the peak regions.

There are at least three ways of improving the situation by using a smoothing formula, say $w_i^* = w_i + \frac{1}{4}\delta^2 w_i$, namely (1) post smoothing: merely smooth the results of the standard DUIT scheme, (2) single smoothing: smooth the results of each upstream sweep before using them in the next downstream sweep, (3) double smoothing: smooth each sweep before being used in the next. Some typical results are presented in Table III. The two values of x chosen are roughly at the smallest and

TABLE III

Comparison of Smoothing Procedures

	$x = 1.3$			$x = 1.64$		
NODS	Post	Single	Double	Post	Single	Double
3	0.0229	0.0229	0.0229	0.1855	0.1855	0.1853
4	0.0234	0.0234	0.0234	0.1851	0.1851	0.1849
5	0.0239	0.0239	0.0239	0.1848	0.1847	0.1845
6	0.0243	0.0243	0.0242	0.1846	0.1844	0.1842
7	0.0245	0.0245	0.0245	0.1844	0.1843	0.1841
8	0.0246	0.0246	0.0246	0.1843	0.1841	0.1840
9	0.0247	0.0246	0.0246	0.1842	0.1841	0.1839

largest values of negative skin friction. Only values from downstream sweeps are given. One must conclude there is little difference between the three results. Since the single smoothing involves only one smoothing every pair of sweeps, produces smooth downstream values and gives more uniform convergence than the standard scheme, we recommend this as the most reliable procedure.

APPENDIX. MATRIX AND VECTOR COMPONENTS FOR SECTION 3.3

The internal details of the 3×3 blocks in (3.8b) are

$$A_j^{n,i} = \begin{pmatrix} -h_j^{-1} & -1/2 & 0 \\ 0 & -h_j^{-1} & -1/2 \\ 0 & 0 & 0 \end{pmatrix} \qquad B_j^{n,i} = \begin{pmatrix} h_j^{-1} & -1/2 & 0 \\ 0 & h_j^{-1} & -1/2 \\ a_{1,j+1}^{n,i} & a_{2,j+1}^{n,i} & a_{3,j+1}^{n,i} \end{pmatrix}$$

$$C_j^{n,i} = \begin{pmatrix} 0 & 0 & 0 \\ 0 & 0 & 0 \\ a_{1,j+1}^{n,i} & a_{2,j+1}^{n,i} & a_{4,j+1}^{n,i} \end{pmatrix} \tag{A1}$$

except that $A_0^{n,i}$ and $C_J^{n,i}$ are irrelevant and

$$B_0^{n,i} = \begin{pmatrix} 1 & 0 & 0 \\ 0 & 1 & 0 \\ a_{1,1}^{n,i} & a_{2,1}^{n,i} & a_{3,1}^{n,i} \end{pmatrix} \qquad B_J^{n,i} = \begin{pmatrix} h_J^{-1} & -1/2 & 0 \\ 0 & h_J^{-1} & -1/2 \\ 0 & -U_J^{n,i} & 0 \end{pmatrix}. \tag{A1}$$

The coefficients in (A1) are:

$$\begin{aligned} a_{1,j}^{n,i} &\equiv [V]_{j-1/2}^{n-1/2,i}\, k_n^{-1}/2, \qquad & a_{3,j}^{n,i} &\equiv -\frac{b_{j-1}^{n,i}}{2} h_j^{-1} + \left[\frac{\partial \psi}{\partial x}\right]_{j-1/2}^{n-1/2,i} \Big/ 4, \\ a_{2,j}^{n,i} &\equiv -\theta [U]_{j-1/2}^{n,i}\, k_n^{-1}/2, \qquad & a_{4,j}^{n,i} &\equiv \frac{b_{j-1}^{n,i}}{2} h_j^{-1} + \left[\frac{\partial \psi}{\partial x}\right]_{j-1/2}^{n-1/2,i} \Big/ 4. \end{aligned} \tag{A2}$$

The inhomogeneous terms have the components

$$\mathbf{r}_j^{n,i} \equiv (r_{j,1}^{n,i}, r_{j,2}^{n,i}, r_{j,3}^{n,i})^T \qquad 0 \leqslant j \leqslant J \tag{A3}$$

where

$$r_{0,1}^{n,i} = -U_0^{n,i}, \quad r_{0,2}^{n,i} = -U_0^{n,i}, \quad r_{J,3}^{n,i} = -\left[\frac{\partial p}{\partial x}\right]_J^{n-1/2,i} - [U]_J^{n-1/2,i} \left[\frac{\partial U}{\partial x}\right]_J^{n-1/2,i} \tag{A4}$$

and

$$\begin{aligned} r_{j-1,3}^{n,i} = &\left[\frac{\partial p}{\partial x}\right]^{n-1/2,i} + \theta [U]_{j-1/2}^{n-1/2,i} \left[\frac{\partial U}{\partial x}\right]_{j-1/2}^{n-1/2,i} - [V]_{j-1/2}^{n-1/2,i} \left[\frac{\partial \psi}{\partial x}\right]_{j-1/2}^{n-1/2,i} \\ &- \left[\frac{\partial (bV)}{\partial y}\right]_{j-1/2}^{n-1/2,i} \end{aligned} \tag{A5}$$

$$r_{j,1}^{n,i} = [U]_{j-1/2}^{n,i} - \left[\frac{\partial \psi}{\partial y}\right]_{j-1/2}^{n,i}, \quad r_{j,2}^{n,i} = [V]_{j-1/2}^{n,i} - \left[\frac{\partial U}{\partial y}\right]_{j-1/2}^{n,i} \quad (1 \leqslant j \leqslant J).$$

REFERENCES

1. S. N. BROWN AND K. STEWARTSON, *Ann. Rev. Fluid Mech.* **1** (1969), 45–72.
2. J. E. CARTER, "Solutions for Laminar Boundary Layers with Separation and Reattachment," AIAA Paper No. 74–583, 1974.
3. J. E. CARTER, "Inverse Solutions for Laminar Boundary-Layer Flows with Separation and Reattachment," NASA TR R-447, 1975.
4. J. E. CARTER AND S. F. WORNUM, *AIAA J.* (8) **13** (1975), 1101–1103.
5. D. CATHERALL AND K. W. MANGLER, *J. Fluid Mech.* (1) **26** (1966), 163–182.
6. T. CEBECI AND P. BRADSHAW, "Momentum Transfer in Boundary Layers," McGraw–Hill/Hemisphere, Washington, 1977.
7. T. CEBECI AND H. B. KELLER, *in* "Proc. 3rd Int. Conf. on Num. Meth. in Fluid Dynam., 1972," Lecture Notes in Physics No. 19, pp. 79–85, Springer–Verlag, Berlin/New York, 1973.
8. T. CEBECI, "Separated Flows and Their Representation by Boundary-Layer Equations," Rept. ONR-CR215-234-2, Mech. Eng. Dept., California State University at Long Beach, 1976.
9. S. GOLDSTEIN, *Quart. J. Mech. Appl. Math.* **1** (1948), 43–69.
10. H. P. HORTON, *AIAA J.* (12) **12** (1974), 1772–1774.
11. H. B. KELLER, *in* "Numerical Solution of Partial-Differential Equations" (J. Bramble, Ed.), Vol. II, Academic Press, New York, 1970.
12. H. B. KELLER AND T. CEBECI, *J. Computational Physics* **10** (1972), 151–161.
13. H. B. KELLER, *SIAM J. Num. Anal.* **11** (1974), 305–320.
14. J. B. KLEMP AND A. ACRIVOS, *J. Fluid Mech.* (1) **53** (1972), 177–191.
15. J. M. KLINEBERG AND J. L. STEGER, "On Laminar Boundary-Layer Separation," AIAA Paper No. 74–94, Jan./Feb., 1974.
16. T. A. REYHNER AND I. FLUGGE-LOTZ, *Int. J. Nonlinear Mech.* (2) **3** (1968), 173–199.
17. P. G. WILLIAMS, *in* "Proceedings of the Fourth International Conf. on Numerical Methods in Fluid Dynamics" (R. D. Richtmyer, Ed.), pp. 445–451, Lecture Notes in Physics No. 35, Springer–Verlag, Berlin/New York, 1975.
18. P. G. WILLIAMS, presented at Specialist's Workshop on Viscous Interaction and Boundary-Layer Separation, Ohio State Univ., Columbus, Ohio, 1976.